Frontiers in Health Informatics
ISSN-Online: 2676-7104
www.healthinformaticsjournal.com
2024; Vol 13: Issue 3
Open Access

Pulsed Laser Ablation Synthesis of TiO2 Nanoparticles and Enhanced Cytotoxicity on Ocular Melanoma Cells via Combined Femtosecond Laser Treatment

Mustafa Ayad [1,2], Safaa Taha [1], Fatma Abdel-Samad [1], Yasmin Abd El-Salam [1], Ahmed O. El-Gendy [1,3*], Tarek Mohamed [1,4]

[1]Laser Institute for Research and Applications LIRA, Beni-Suef University, Beni-Suef 62511, Egypt
[2]Diyala Health Department, Ministry of Health, Iraq
dr.mustfa91@gmail.com
[3]Faculty of Pharmacy, Department of Microbiology and Immunology, Beni-Suef University, Beni-Suef 62514, Egypt
[4]Department of Engineering, Faculty of Advanced Technology and Multidiscipline, Universitas Airlangga, Indonesia
*Corresponding author: E-mail: ahmed.elgendy@pharm.bsu.edu.eg

Cite this paper as: Mustafa Ayad, Safaa Taha, Fatma Abdel-Samad, Yasmin Abd El-Salam, Ahmed O. El-Gendy, Tarek Mohamed (2024) Pulsed Laser Ablation Synthesis of TiO2 Nanoparticles and Enhanced Cytotoxicity on Ocular Melanoma Cells via Combined Femtosecond Laser Treatment. *Frontiers in Health Informatics, 13* (3), 9651-9663

Abstract
The development of innovative nanomaterials has gained momentum in the biomedical field, particularly for therapeutic applications. The synthesis of titanium dioxide (TiO_2) nanoparticles was achieved using pulsed laser ablation (PLA) in liquid, offering a method to generate ultrapure nanoparticles with well-controlled size and morphology, eliminating the need for chemical precursors. Characterization via high-resolution transmission electron microscopy (HR-TEM) confirmed spherical nanoparticles, with average sizes ranging from 6.4 nm to 19.1 nm, determined by the length of the ablation process. In vitro cytotoxicity was evaluated using an MTT assay, where the A375 cells were treated with various concentrations of TiO_2 nanoparticles, both alone and in combination with femtosecond laser irradiation. The results demonstrated a significant enhancement in cytotoxicity when the cells were exposed to the combined treatment, compared to either treatment alone. This suggests that the synergistic effect of TiO_2 nanoparticles and femtosecond laser irradiation may provide a more effective therapeutic strategy for targeting ocular malignant melanoma cells. In addition, the antioxidant activity of TiO_2 nanoparticles was evaluated through the DPPH free radical scavenging assay, demonstrating mild antioxidant properties, which may contribute to their enhanced therapeutic potential. This report underscores the potential of pulsed laser ablation as a scalable method for producing biocompatible nanoparticles and highlights the promise of combining these nanoparticles with femtosecond laser treatment for the development of advanced cancer therapies.

Keywords: *Pulsed Laser Ablation; TiO_2 Nanoparticles; Ocular Malignant Melanoma; Femtosecond Laser Irradiation; Cytotoxicity; Antioxidant Activity*

1. Introduction

Nanotechnology, which involves the study and application of materials with dimensions ranging from 1 to 100 nanometers, has revolutionized various fields, including medicine, due to the exceptional properties of nanoparticles (NPs) [1]. Among these, titanium dioxide (TiO2) nanoparticles have fascinated substantial consideration for their diverse applications, particularly in the biomedical sciences [2]. TiO2 NPs possess a great surface to volume ratio, remarkable photocatalytic activity, and chemical stability, making them ideal candidates for diverse medical applications, including drug delivery, diagnostic imaging, and as antitumor agents [3]. In ophthalmology, the unique properties of TiO2 NPs offer significant potential, particularly in overcoming the challenges associated with drug delivery to ocular tissues [4]. Barriers such as the corneal epithelium, tear film, and blood-retina barrier complicate the delivery of therapeutic agents to the eyes, driving the exploration of NP-based carriers for more effective treatment [5]. For instance, NPs can be employed more successfully to deliver poorly water-soluble compounds, like cyclosporine or glucocorticoids, which are utilized to treat immunological or vision-threatening eye illnesses [6]. Adsorption of medicines such as phenytoin and 5-FU onto metal and oxide nanoparticles can aid in wound healing and cancer treatment [7].

TiO2 NPs, capable of penetrating cellular membranes and epithelial barriers, show promise as vehicles for targeted drug delivery in treating ocular diseases like diabetic retinopathy and age-related macular degeneration [8]. Additionally, their photo-reactive properties make them potential candidates for photodynamic therapy (PDT) in treating ocular malignancies, such as malignant melanoma [9].

Malignant melanoma of the eye, though less common than its cutaneous counterpart, poses a severe threat to vision and life, especially when it metastasizes [10]. Conventional treatments, including surgery, radiotherapy, and chemotherapy, often have limited effectiveness and cause significant side effects [11]. As a result, there is growing interest in alternative treatments that offer better targeting of tumor cells while minimizing damage to surrounding healthy tissues. In this context, TiO2 NPs combined with laser therapy emerge as a promising approach for treating ocular malignant melanoma [12].

The synthesis of TiO2 NPs has traditionally relied on commercial methods such as sol-gel processing, hydrothermal techniques, and chemical vapor deposition (CVD) [13]. While these methods have been effective in producing TiO2 NPs on a large scale, they also present significant drawbacks, particularly in terms of scalability, purity, and complexity [14]. For instance, the sol-gel method, despite offering control over particle size and morphology, often requires high-temperature processing and the use of organic solvents, leading to impurities and complicating the purification process [15]. Hydrothermal synthesis, although producing well-crystallized nanoparticles with controlled morphology, necessitates specialized equipment and long reaction times under high-pressure conditions, which pose safety risks and potential contamination from surfactants [16]. Similarly, CVD offers excellent control over film thickness and uniformity but requires high temperatures, expensive precursors, and complex equipment, limiting its scalability and increasing production costs [17].

Given the limitations of these conventional methods, there has been a growing interest in alternative approaches that overcome these challenges. Pulsed laser ablation in liquid (PLAL) has developed as a favorable method for the production of ultrapure TiO2 NPs without the need for chemical precursors, surfactants, or high-temperature processing [18]. This technique involves directing a high-energy laser pulse onto a solid titanium object submerged in liquid, resulting in the ablation of the material and the formation of nanoparticles [19]. The laser ablation process is highly versatile, performed under ambient conditions, and allows for precise control over nanoparticle size and morphology by adjusting laser parameters, making it simpler and more cost-effective than conventional methods [20].

One of the key advantages of PLAL is the production of ultrapure nanoparticles. The absence of chemical reagents during synthesis ensures that the resulting TiO2 NPs are free from contaminants and byproducts, crucial for biomedical purposes such as drug delivery and cancer treatment [21]. Moreover, PLAL enables the making of a varied collection of nanoparticle sizes and shapes, from spherical particles to nanorods and nanowires, by tuning laser conditions and the properties of the liquid medium [22]. This versatility, combined with

the inherent purity of the produced nanoparticles, positions PLAL as an attractive method for producing high-quality TiO2 NPs suitable for sensitive applications like biomedicine. [23].
This study aims to synthesize high-purity TiO_2-NPs using pulsed laser ablation and to evaluate their cytotoxic effects on ocular malignant melanoma cells.

2. Methodology

2.1. Laser ablation and production of TiO_2-NPs

TiO_2-NPs were synthesized by means of a laser ablation method applied to a bulk titanium plate submerged in distilled water (DW), as shown in **Fig 1**. The titanium target was a rectangular plate with dimensions of 20 × 40 × 2 mm and a purity of 99.99%. Before ablation, the titanium surface was polished to detach the oxide deposit formed through air exposure, ensuring a smooth, clean surface free of protrusions. The plate was then washed with alcohol and deionized water, followed by ultrasonic cleaning for 30 minutes to eliminate any organic residues. The titanium plate was immersed in a glass beaker containing 10 mL of purified water using a holder. To prevent particulate matter from obstructing the laser path and absorbing the incident energy, the beaker was placed on a speed-controlled stirrer, ensuring solution homogenization. For the ablation process, a second harmonic Nd: YAG laser system from Spectra-Physics (Quanta-Ray PRO 350) was employed, featuring a wavelength of 532 nm, a pulse duration of 10 ns, and a repetition rate of 10 Hz. The laser beam was directed onto the titanium surface using highly reflective mirrors, with an L-convex lens of 10.5 cm focal length focusing the beam. To ensure colloid homogenization, prevent particle interference with the laser path, and avoid deterioration during ablation, the sample beaker was rotated at 177 rounds per minute (RPM) using a motorized spinner. The effects of varying ablation times on the synthesized NPs were investigated at ablation times ranging from 5 to 20 minutes and at an average laser power of 150 mW. The synthesized TiO2 nanoparticles (TiO2 NPs) are characterized for their structural, optical, and physical properties, elemental composition, and NP concentrations through various techniques, including transmission electron microscopy (TEM), ultraviolet-visible absorption spectroscopy (UV-Vis), energy dispersive X-ray (EDX) analysis, and inductively coupled plasma (ICP).

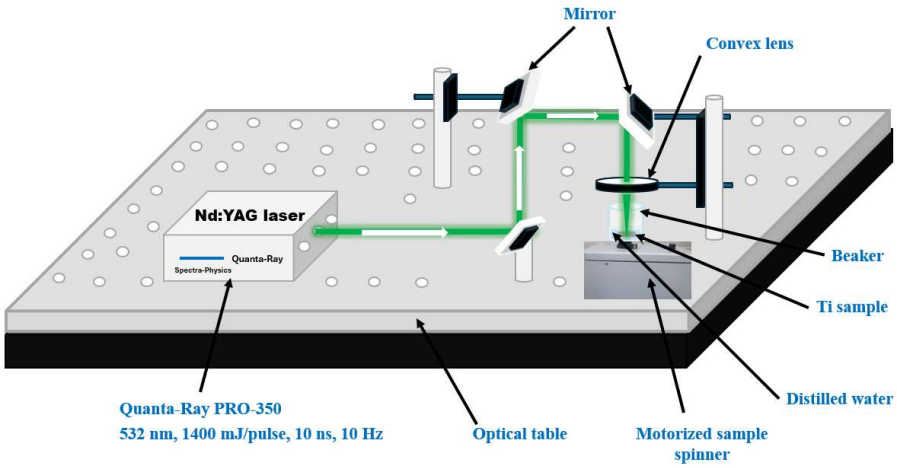

Figure 1. A schematic diagram illustrating the laser ablation in liquid for synthesizing TiO2 nanoparticles (TiO2-NPs) using the second harmonic of the Nd: YAG laser at a wavelength of 532 nm in pulsed mode.

2.2. Cell Culture and TiO_2-NPs Treatment

This study utilized the human cancerous melanoma cell line A375 (ATCC® CRL-1619™). Pre-warmed DMEM medium (Biowest) was used to culture the cells, enriched with 10% fetal bovine serum (Gibco, USA) and 1% penicillin/streptomycin. This supplementation ensured ideal conditions for cell growth. They were incubated at

37°C under 5% CO2 and high humidity conditions. Subcultures were observed at roughly 80–90% confluence using an inverted fluorescence microscope (Leica, DMi8). The cells were then plated at a density of 10,000 cells per well in 96-well plates. 24-hour after seeding, the concentration of TiO_2 (nanoparticles synthesized via laser ablation) (6 µg/mL) was added to the cells at a final concentration of 2.4 µg/mL. Other wells were subjected to femtosecond laser treatment, either in the presence or absence of TiO2-NPs. An MTT assay was then performed on all wells, including a control that received neither TiO2-NPs nor femtosecond laser treatment.

2.3. Femtosecond Laser System Setup and Cytotoxicity Assessment Using MTT Assay

The human malignant melanoma A375 cell line was exposed to tunable femtosecond laser light, utilizing a mode-locked femtosecond Ti: sapphire MAI TAI HP laser (Spectra-Physics). Operating with an average power between 1.5 and 2.9 W, a repetition rate of 80 MHz, and a wavelength range from 690 to 1040 nm, this laser system provided pulses to the INSPIRE HF100 laser (Spectra-Physics). A notable characteristic of the INSPIRE HF100 laser system is its ability to adjust wavelengths. In addition to the standard infrared pump wavelengths, the system can also function in OPO or SHG modes. When Ti: sapphire laser is tuned and the potassium dihydrogen phosphate (KDP) second harmonic nonlinear crystal is rotated, the SHG mode produces output within a wavelength range of 345–520 nm. Simultaneously, the OPO mode generates a signal between 490–750 nm and an idler between 930–2500 nm by tuning Lithium Niobate (LN) crystals. The system allowed for wavelength tuning from 345 to 2500 nm, with output distributed through four exit apertures. The power of the laser beam was measured using a Newport 843R power meter. As shown in **Fig. 2**, the laser beam was located approximately 10 cm above each well in a covered 96-well plate, safeguarding the cells from environmental contamination during irradiation. Using a beam expander composed of two converging lenses, the initial beam diameter of approximately 2 mm was increased to about 20 mm. The beam diameter was further adjusted using an iris, while a laser attenuator controlled the intensity directed at the cells. The laser beam was focused on the cells using highly reflective mirrors, as illustrated in **Fig.2.** The femtosecond laser light was delivered to the cells at specific wavelengths of 420 nm. Because of a 14% loss of laser power during transmission through the cover of the 96-well plate, only 100 mW of laser power was successfully delivered to the cells, which required an input irradiation power of 114–116 mW.

The impact of TiO2-NP treatment, femtosecond laser irradiation, and their combined effects on cell proliferation was examined using the 3-[4,5-dimethylthiazol-2-yl]-2,5-diphenyl tetrazolium bromide (MTT) assay. The principle of this assay relies on the ability of mitochondrial enzymes in viable cells to reduce the yellow MTT dye, resulting in the formation of purple formazan crystals. This conversion links total mitochondrial activity to the number of viable cells, thereby making it a standard technique for assessing cell growth *in vitro*. MTT powder was dissolved in PBS to create a 5 mg/mL stock solution (Life Technologies Corporation, M6494), stored at 4°C, and protected from light. Following 24 hours of laser irradiation, the media was removed, and each well received 110 µL of MTT solution diluted in DMEM at a 1:10 ratio. The plates were incubated at 37°C for three hours. After incubation, the MTT-containing media was discarded, and the plates were agitated for 12 minutes. Following this, 100 µL of DMSO was introduced to dissolve the formazan crystals, and the plates were subsequently incubated in a CO2 incubator for 15 minutes. After this incubation, the plates were agitated on a plate shaker for three minutes, and the absorbance was then measured at 570 nm using an ELISA reader.

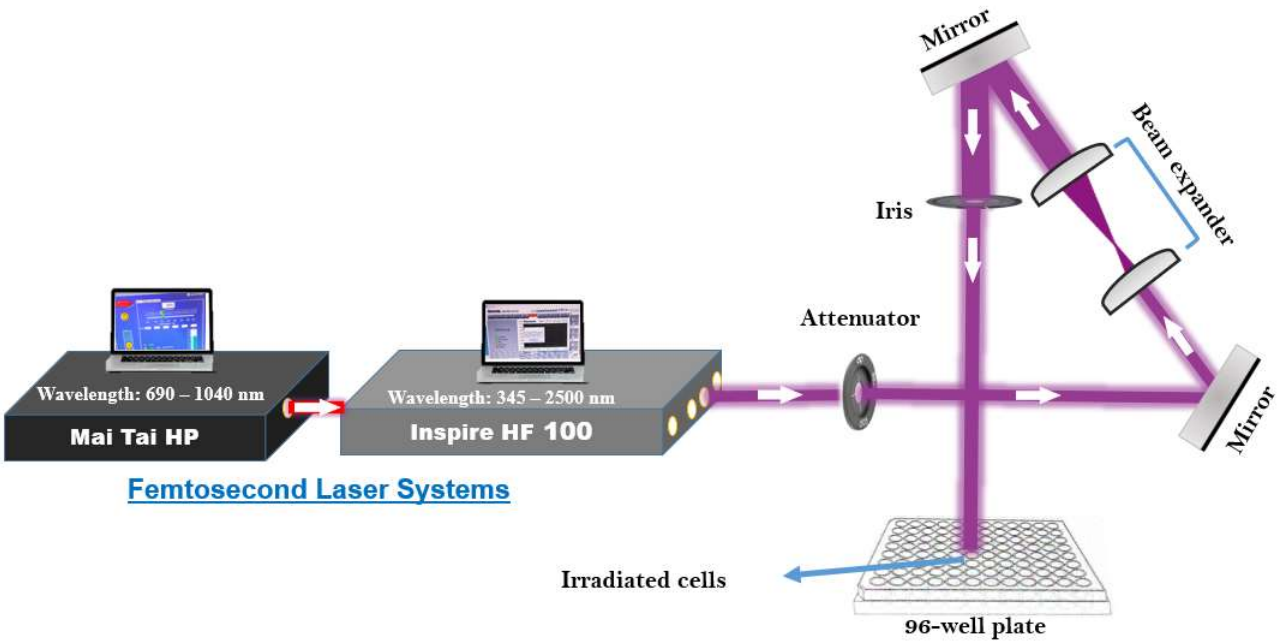

Figure 2. Schematic illustration of the A375 cell irradiation experimental setup

2.4. Exploring Antioxidant Activities Using DPPH (2,2-Diphenyl-1-picrylhydrazyl) Free Radical Scavenging Assay

A 2 mM Trolox standard solution was prepared for the DPPH assay. From this stock solution, final concentrations of 80, 60, 50, 40, 35, 30, 25, 20, and 15 µM were prepared in distilled water. TiO_2-NPs samples at concentrations of 3 µg/mL, 2.175 µg/mL, 1.45 µg/mL, and 0.95 µg/mL were also prepared and analyzed after vortexing.

The evaluation of DPPH free radical scavenging activity followed the method outlined by Boly et al. (2016) [24], incorporating modifications from Elkholy et al. (2023) [25]. Initially, 100 µL of freshly prepared DPPH reagent (0.1% in methanol) was combined with 100 µL of the sample in a 96-well plate. The mixture was incubated in the dark at room temperature for 30 minutes. After incubation, the reduction in DPPH color intensity was measured at 540 nm. Results are expressed as means ± SD and calculated using the formula: percentage inhibition = ((Average absorbance of blank - Average absorbance of the test) / (Average absorbance of blank)) × 100.

The measurements were taken with a FluoStar Omega microplate reader. The DPPH reducing capacity of the TiO2-NP samples is reported as µM Trolox Equivalent (TE) per mL of sample, based on the linear regression equation derived from the Trolox calibration curve.

2.5. Statistical analysis

Data are expressed as means ± standard errors of the mean (SEM) from three independent experiments, each performed in quadruplicate. A P-value of less than 0.05 was deemed statistically significant. For assessing differences between groups, Tukey's multiple comparisons test and one-way analysis of variance (ANOVA) were utilized, with GraphPad Prism (version 5) for analysis.

3. Results and discussion

3.1. Characterization of TiO_2-NPs colloids

3.1.1. TiO_2NPs shape and particle size distribution analysis by TEM

Figure 3 shows TEM images of the particle size distribution and shape of TiO_2 NPs synthesized via laser ablation. A high-resolution TEM image exhibited the spherical morphology of the colloidal TiO_2 NPs at different ablation times and an ablation laser fluence of 1.24 J/cm^2. The density of NPs increases with increasing ablation time, as shown in **Fig. 3**. Because of increased ablation time, more NPs are formed. Figure 3 depicts that the size distribution histogram and average sizes of TiO_2 NP colloids are 19.11 nm, 11.96 nm, 8.33 nm, and 6.4 nm, for laser ablation times of 5, 10, 15, and 20 minutes respectively. The size of spherical NPs decreases as laser ablation time increases. Because laser ablation produces NPs that are dispersed in the solution, most of them will be irradiated by the laser, causing size reduction. The reduction in NP size can be attributed to photofragmentation caused by laser ablation.

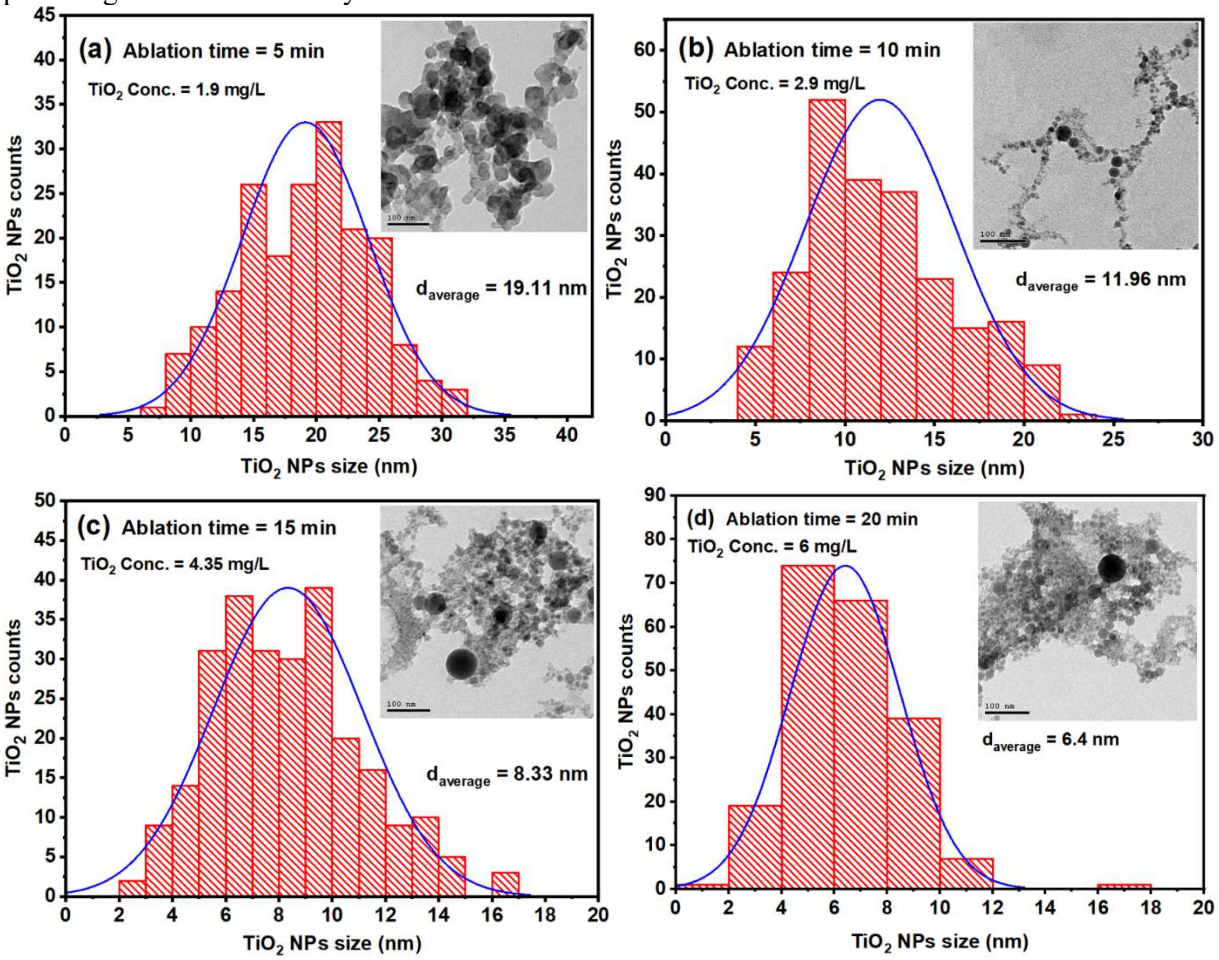

Figure 3: Size distribution of TiO_2NPs synthesized via laser ablation with an average laser power of 150 mW, using different ablation times: (a) 5 minutes, (b) 10 minutes, (c) 15 minutes, and (d) 20 minutes. The inset shows the TEM images of TiO_2 NPs.

3.1.2. Optical absorption characteristics of TiO_2-NPs using UV-Vis spectroscopy

The optical absorption of TiO_2 NPs was measured using a UV-Vis spectrophotometer (Model: C-7200) with a wavelength range of 200–1100 nm, as shown in **Fig. 4**. The absorption spectrum shows that the TiO_2 colloidal

solutions absorb light strongly in the UV region. Absorbance intensity reflects the concentration of NPs in the solution. According to the Beer-Lambert law, the amount of light absorbed is proportional to the substance's concentration. As the ablation time increases, the absorbance of TiO_2 NPs increases, indicating that there are more NPs in the solution at an ablation time of 20 min. Colloidal TiO_2NPs exhibit a surface plasmon resonance (SPR) peak around the 227 nm region. The size, shape, and concentration of TiO_2NPs can all affect the position of the SPR peak. With increasing laser ablation time, the peak position shifts toward a shorter wavelength due to the synthesis of smaller particle sizes. The SPR peaks also became sharper as the ablation time increased, as seen with the 20 min ablation time.

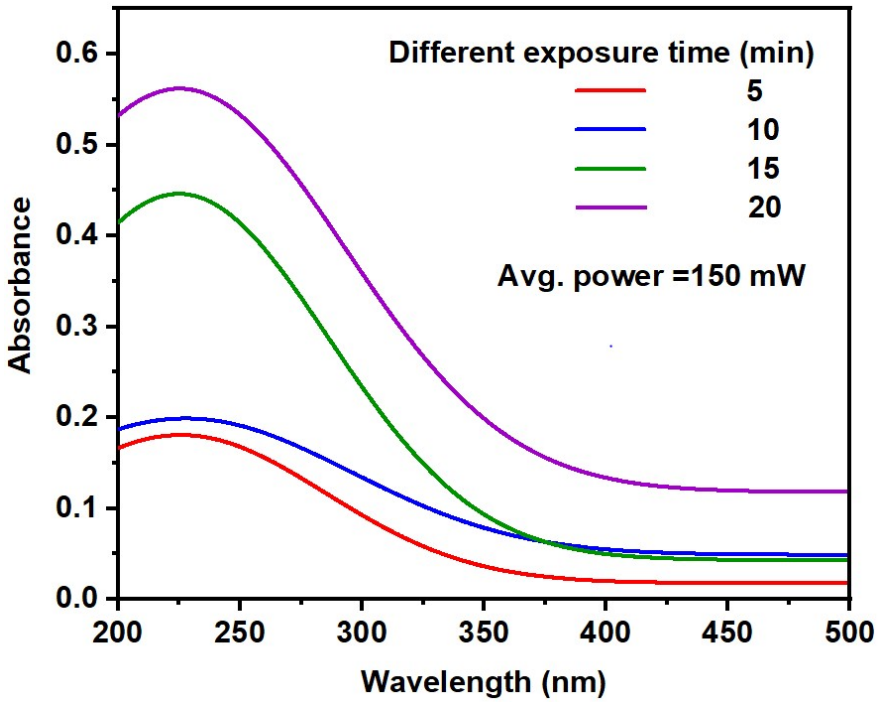

Figure 4: The absorption spectrum of TiO_2 NP colloidal solutions at different ablation times and a constant average power of 150 mW.

3.1.3. Elemental analysis of TiO_2-NPs using EDX

The elemental analysis of the titanium dioxide NPs colloidal solution in distilled water was studied using energy-dispersive X-ray spectroscopy (EDX) JSM6510LA Eds detector Oxford. EDX results depict the presence of titanium (Ti) and oxygen (O), with their respective atomic and weight fractions detailed in the EDX spectrum, as shown in **Fig. 5**. We used the ZAF method to determine the atomic composition of TiO_2 NP colloids, where Z stands for atomic number, A for absorption, and F for fluorescence. **Table 1** summarizes the results, showing the atomic and weight ratios of Ti and O in the solution. This analysis confirms the high purity of the synthesized TiO_2 NPs, indicating the absence of significant impurity elements.

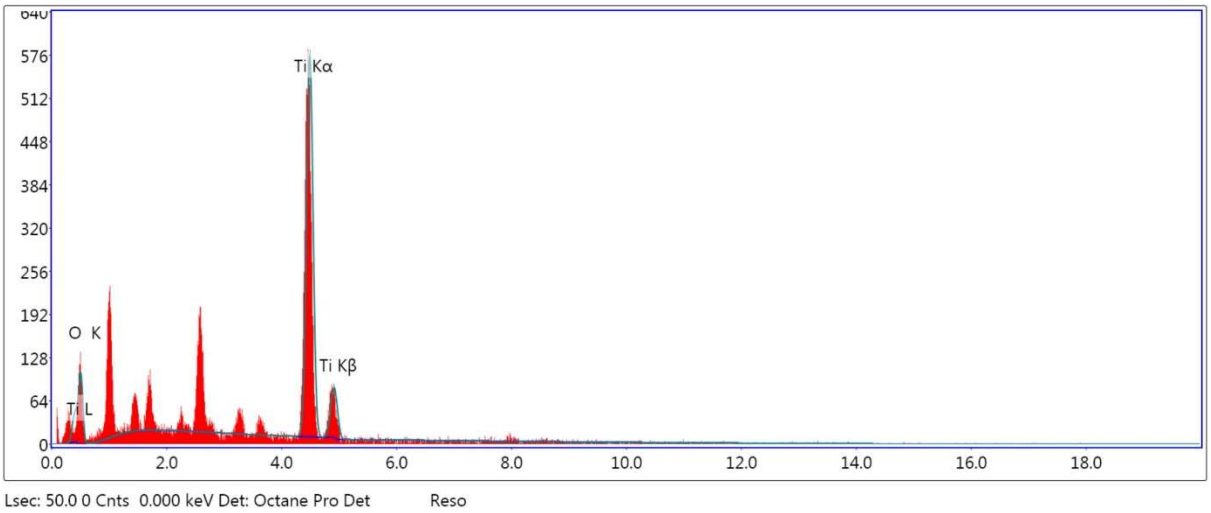

Figure 5: The EDX spectra of TiO2 NPs reveal peaks for the majority of the elements present.

Table 1. ZAF Method Standardless Quantitative Analysis of TiO_2 NP colloids

Element	Weight %	Atomic %	Error %
Ti K	57.94	31.51	2.78
O K	42.06	68.49	14.01

3.1.4. TiO_2 NPs concentration measurements using ICP

The concentration of TiO2 NP colloids produced at different ablation times—5, 10, 15, and 20 minutes—was measured using inductively coupled plasma (ICP) (Agilent 5100 Synchronous Vertical Dual View (SVDV) ICP–OES, Agilent Vapor Generation Accessory VGA 77), as shown in **Table 2**. The findings revealed that increasing the ablation time from 5 to 20 minutes led to a rise in TiO2 NP colloid concentration from 1.9 to 6 mg/L, indicating that longer ablation times result in enhanced ablation efficiency.

Table 2: TiO_2 NPs concentration measured using the ICP technique.

NPs sample	Ablation time (min)	Concentration (mg/L)
TiO_2 NPs	5	1.9
	10	2.9
	15	4.35
	20	6

3.2. MTT assay and determination of cell viability

The MTT assay results revealed that the percentage of viable ocular melanoma cells relative to the control was 36.5% for femtosecond laser treatment at 420 nm and 19.7% for the combination of TiO_2 nanoparticles with femtosecond laser treatment at 420 nm, as shown in **Fig. 6**. In contrast, there was no significant difference in cell viability between the control group and cells treated exclusively with TiO2 nanoparticles. Therefore, the combination of TiO2 nanoparticles and femtosecond laser treatment was more effective in reducing cell viability than either treatment alone. A prior study indicated that nitrogen-doped titanium dioxide (N-TiO2) nanoparticles (NPs) at concentrations of 1 and 100 µg/ml did not significantly alter ROS levels in A375 cells or only caused

a slight increase [26]. Additionally, previous research has shown that TiO2-NPs can negatively impact cell viability, proliferation, and the cell cycle [27, 28].

Femtosecond laser irradiation at 420 nm significantly decreased A375 cell viability compared to control cells. This observation is consistent with earlier findings that reported a reduction in T47D cell viability to 44.4% following exposure to 420 nm femtosecond laser irradiation [29]. Recent studies have suggested that blue light can induce the formation of oxygen radicals in skin cells [30]. Possible absorption by cytochrome c oxidase (CCO) may explain these results, as CCO has absorption peaks at 418–420 nm and 598–600 nm, showing minimal absorption in the red-near infrared spectrum [31]. In line with this, Wang et al. demonstrated that exposure to blue LED light (415 nm, 16 mW/cm²) caused significant reductions in intracellular ATP levels, mitochondrial membrane potential, and intracellular pH, while increasing intracellular ROS in human adipose stem cells [32]. Furthermore, previous studies reported that CCO's absorbance for blue light (415 nm) and green light (540 nm) is about 20 and 3 times higher, respectively, than that for 670 nm [33]. Liebmann et al. found that exposure of human skin cells to high fluences of blue light (412–426 nm) over a duration of up to 3 days led to cell death via apoptosis in a dose-dependent manner [34].

The photodynamic effect of TiO2 has been established for both UV light and the entire visible spectrum [35, 36]. TiO2 has garnered considerable interest as a photosensitizer for photodynamic therapy (PDT) in cancer treatment, primarily due to its capability to generate ROS upon light irradiation [27].

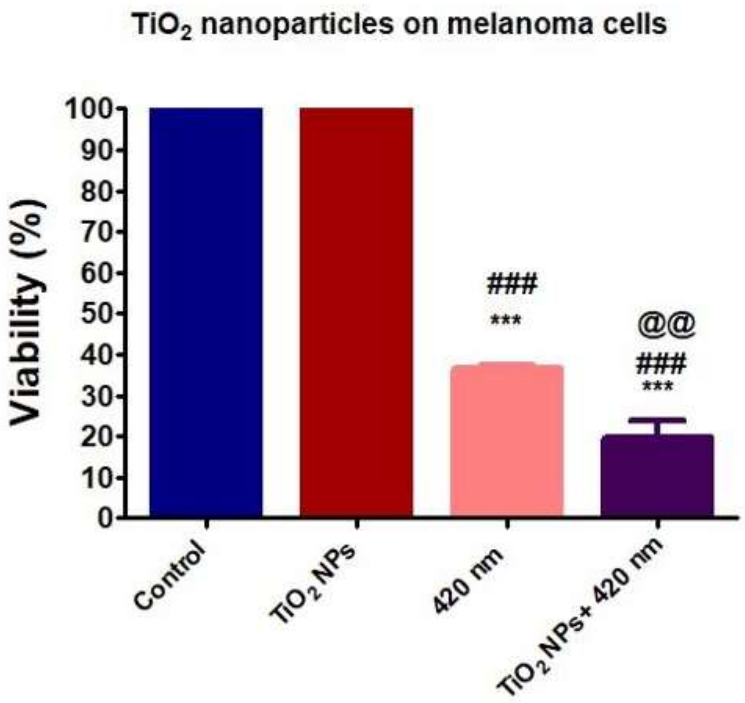

Figure 6: Effects of 420 nm femtosecond laser irradiation and TiO2-NPs on the viability of ocular melanoma A375 cells, assessed 24 hours post-treatment. Cell viability was determined using the MTT assay and is presented as a percentage relative to untreated control cells. Statistical significance is indicated as follows: * significant difference from the control; # significant difference from TiO2-NPs; @ significant difference from 420 nm treatment. *P < 0.05, **P < 0.01, and ***P < 0.001.

3.3. Antioxidant Activity

The Trolox Equivalent Antioxidant Capacity (TEAC) assay measures antioxidant activity by determining the scavenging of DPPH (2,2-Diphenyl-1-picrylhydrazyl) free radicals, which are converted into a colorless product during this reaction The extent of decolorization induced by TiO_2 nanoparticles (NPs) was compared to that caused by Trolox. The linear regression equation derived from the relationship between various Trolox concentrations (µM) and the percentage of radical scavenging activity **(Fig. 7a)** was used to estimate the Trolox equivalent amounts for each TiO_2-NP concentration and the results are expressed as µM TE/mg.

As shown in Fig. 7b, TiO2 NPs demonstrated weak, dose-dependent antioxidant activity, with a concentration of 3 µg/mL resulting in 5.94% antioxidant activity, equivalent to 17.88 µM Trolox per mg of sample [25]. Although the antioxidant capacity of TiO2 NPs is modest, it remains a valuable feature for mitigating oxidative stress by neutralizing excess reactive oxygen species (ROS) and free radicals. This capability is important for maintaining cellular health and suggests that TiO2 NPs, along with other nanoparticles, could be partially effective in reducing oxidative stress. TiO2 NPs exposure in HepG2 cells resulted in increases in intracellular GSH levels that were both dose-dependent and time-dependent [37]. Conversely, a recent study by Gerloff et al. [38] found that when Caco-2 cells were exposed to TiO2 NPs (which consisted of 80% anatase and 20% rutile) for 4 hours, the GSH content remained unchanged. Additionally, Horie et al. [39] found a significant decrease in intracellular GSH levels in human keratinocyte HaCaT cells after 24 hours of exposure to nanosized TiO2, whereas fine-sized TiO2 particles did not show the same impact.

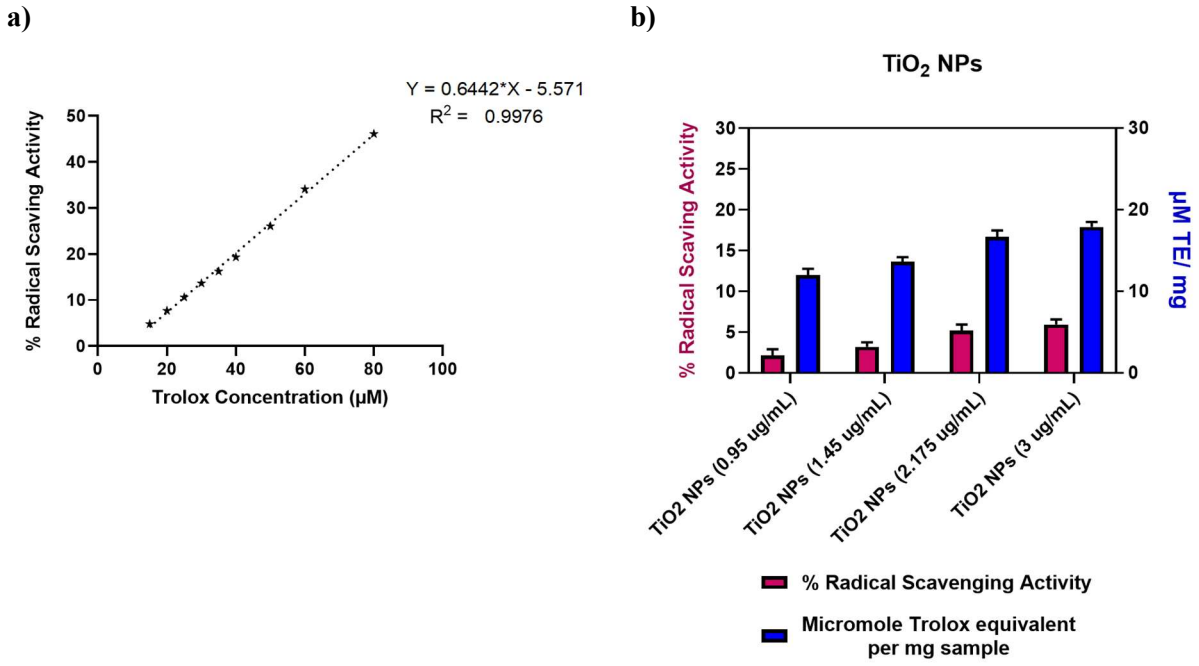

Figure 7: Antioxidant activity of TiO2-NPs assessed using the DPPH free radical scavenging assay. Panel (a) illustrates the relationship between various Trolox concentrations (µM) and the corresponding percentage of free radical scavenging activity. Panel (b) depicts the antioxidant activity of different concentrations of TiO2-NPs, represented both as a percentage of radical scavenging activity and in terms of µM Trolox equivalent (TE) per mg of sample.

Conclusion

The findings of this study underscore the effectiveness of pulsed laser ablation as a precise and clean technique for synthesizing TiO_2-NPs, offering significant advantages over conventional methods. The synthesized nanoparticles demonstrated notable cytotoxic effects against A375 ocular malignant melanoma cells, particularly when combined with femtosecond laser treatment, indicating promising potential for cancer therapy applications. Furthermore, the TiO_2-NPs exhibited considerable antioxidant activity, suggesting additional therapeutic benefits in mitigating oxidative stress. This dual approach of nanoparticle synthesis and laser treatment could pave the way for innovative therapies in ocular melanoma and possibly other malignancies. Future research should focus on optimizing laser parameters, exploring nanoparticle surface modifications, and conducting *in vivo* testing to fully harness the therapeutic potential of this approach. Ensuring the safety and efficacy of this treatment method through rigorous preclinical and clinical trials will be crucial for its potential application in human therapies.

Author Contributions: Conceptualization, Tarek Mohamed, Ahmed O. El-Gendy and Ola Dabbous; methodology, Emad Neamah, Yasmin Abd El-Salam, Esraa Ahmed, Fatma Abdel-Samad; validation, Emad Neamah, Tarek Mohamed and Ahmed O. El-Gendy; formal analysis, Yasmin Abd El-Salam, Esraa Ahmed and Fatma Abdel-Samad; writing—original draft preparation, Emad Neamah, Yasmin Abd El-Salam, Esraa Ahmed, Fatma Abdel-Samad; writing—review and editing, Tarek Mohamed, and Ahmed O. El-Gendy; supervision, Tarek Mohamed, Ola Dabbous and Ahmed O. El-Gendy; project administration, Tarek Mohamed; All authors have read and agreed to the published version of the manuscript.

Funding: This research received no external funding.
Conflicts of Interest: The authors declare no conflict of interest.

References

1. Patel JK, Patel A and Bhatia D. Introduction to nanomaterials and nanotechnology. *Emerging technologies for nanoparticle manufacturing*. Springer, 2021, pp.3-23.
2. Yin ZF, Wu L, Yang HG, et al. Recent progress in biomedical applications of titanium dioxide. *Physical chemistry chemical physics* 2013; 15: 4844-4858.
3. Akakuru OU, Iqbal ZM and Wu A. TiO2 nanoparticles: properties and applications. *TiO2 Nanoparticles: Applications in Nanobiotechnology and Nanomedicine* 2020: 1-66.
4. Gabai A, Zeppieri M, Finocchio L, et al. Innovative strategies for drug delivery to the ocular posterior segment. *Pharmaceutics* 2023; 15: 1862.
5. Suri R, Beg S and Kohli K. Target strategies for drug delivery bypassing ocular barriers. *Journal of drug delivery science and technology* 2020; 55: 101389.
6. Dimakis AC. Nanotechnology in Ophthalmology, new developments. 2020.
7. de Sousa Victor R, Marcelo da Cunha Santos A, Viana de Sousa B, et al. A review on Chitosan's uses as biomaterial: Tissue engineering, drug delivery systems and cancer treatment. *Materials* 2020; 13: 4995.
8. Lyu Q, Peng L, Hong X, et al. Smart nano-micro platforms for ophthalmological applications: The state-of-the-art and future perspectives. *Biomaterials* 2021; 270: 120682.
9. Rodriguez-Devora JI, Ambure S, Shi Z-D, et al. Physically facilitating drug-delivery systems. *Therapeutic delivery* 2012; 3: 125-139.
10. Brownstein S. Malignant melanoma of the conjunctiva. *Cancer Control* 2004; 11: 310-316.
11. Debela DT, Muzazu SG, Heraro KD, et al. New approaches and procedures for cancer treatment: Current perspectives. *SAGE open medicine* 2021; 9: 20503121211034366.
12. Mariano S, Carata E, Calcagnile L, et al. Recent Advances in Photodynamic Therapy: Metal-Based Nanoparticles as Tools to Improve Cancer Therapy. *Pharmaceutics* 2024; 16: 932.

13. Akinnawo S. Synthesis, modification, applications and challenges of titanium dioxide nanoparticles. *Research Journal of Nanoscience and Engineering* 2019; 3: 10-22.
14. Petronella F, Truppi A, Dell'Edera M, et al. Scalable synthesis of mesoporous TiO2 for environmental photocatalytic applications. *Materials* 2019; 12: 1853.
15. Niederberger M and Pinna N. *Metal oxide nanoparticles in organic solvents: synthesis, formation, assembly and application*. Springer Science & Business Media, 2009.
16. Mosayebi J, Kiyasatfar M and Laurent S. Synthesis, functionalization, and design of magnetic nanoparticles for theranostic applications. *Advanced Healthcare Materials* 2017; 6: 1700306.
17. Sun L, Yuan G, Gao L, et al. Chemical vapour deposition. *Nature Reviews Methods Primers* 2021; 1: 5.
18. Makarov GN. Laser applications in nanotechnology: nanofabrication using laser ablation and laser nanolithography. *Physics-Uspekhi* 2013; 56: 643.
19. Zeng H, Du XW, Singh SC, et al. Nanomaterials via laser ablation/irradiation in liquid: a review. *Advanced Functional Materials* 2012; 22: 1333-1353.
20. Fazio E, Gökce B, De Giacomo A, et al. Nanoparticles engineering by pulsed laser ablation in liquids: Concepts and applications. *Nanomaterials* 2020; 10: 2317.
21. Hamrayev H, Korpayev S and Shameli K. Advances in Synthesis Techniques and Environmental Applications of TiO2 Nanoparticles for Wastewater Treatment: A Review. *Journal of Research in Nanoscience and Nanotechnology* 2024; 12: 1-24.
22. Selvaraj A, Parangusan H, Vikraman D, et al. Metal nanoparticles and alloys produced by pulsed laser ablation in liquids for photocatalytic remediation. *Pulsed Laser-Induced Nanostructures in Liquids for Energy and Environmental Applications*. Elsevier, 2024, pp.87-110.
23. Attallah AH, Abdulwahid FS, Ali YA, et al. Effect of liquid and laser parameters on fabrication of nanoparticles via pulsed laser ablation in liquid with their applications: a review. *Plasmonics* 2023; 18: 1307-1323.
24. Boly R, Lamkami T, Lompo M, et al. DPPH free radical scavenging activity of two extracts from Agelanthus dodoneifolius (Loranthaceae) leaves. *International Journal of Toxicological and Pharmacological Research* 2016; 8: 29-34.
25. Elkholy NS, Hariri MLM, Mohammed HS, et al. Lutein and β-carotene characterization in free and nanodispersion forms in terms of antioxidant activity and cytotoxicity. 2023; 18: 1727-1744.
26. Mohammadalipour Z, Rahmati M, Khataee A, et al. Differential effects of N-TiO2 nanoparticle and its photo-activated form on autophagy and necroptosis in human melanoma A375 cells. 2020; 235: 8246-8259.
27. Çeşmeli S and Biray Avci CJJodt. Application of titanium dioxide (TiO2) nanoparticles in cancer therapies. 2019; 27: 762-766.
28. Hou Y, Cai K, Li J, et al. Effects of titanium nanoparticles on adhesion, migration, proliferation, and differentiation of mesenchymal stem cells. 2013: 3619-3630.
29. Taha S, Mohamed WR, Elhemely MA, et al. Tunable femtosecond laser suppresses the proliferation of breast cancer in vitro. 2023; 240: 112665.
30. Regazzetti C, Sormani L, Debayle D, et al. Melanocytes sense blue light and regulate pigmentation through opsin-3. 2018; 138: 171-178.
31. Malatesta F, Antonini G, Sarti P, et al. Structure and function of a molecular machine: cytochrome c oxidase. 1995; 54: 1-33.
32. Wang Y, Huang Y-Y, Wang Y, et al. Red (660 nm) or near-infrared (810 nm) photobiomodulation stimulates, while blue (415 nm), green (540 nm) light inhibits proliferation in human adipose-derived stem cells. 2017; 7: 1-10.

33. Mason MG, Nicholls P and Cooper CEJBeBA-B. Re-evaluation of the near infrared spectra of mitochondrial cytochrome c oxidase: implications for non invasive in vivo monitoring of tissues. 2014; 1837: 1882-1891.
34. Liebmann J, Born M and Kolb-Bachofen VJJoID. Blue-light irradiation regulates proliferation and differentiation in human skin cells. 2010; 130: 259-269.
35. Xie X, Mao C, Liu X, et al. Synergistic bacteria killing through photodynamic and physical actions of graphene oxide/Ag/collagen coating. 2017; 9: 26417-26428.
36. Tatlıdil İ, Sökmen M, Breen C, et al. Degradation of C andida albicans on TiO 2 and Ag-TiO 2 thin films prepared by sol–gel and nanosuspensions. 2011; 60: 23-32.
37. Petković J, Žegura B and Filipič M. Influence of TiO2 nanoparticles on cellular antioxidant defense and its involvement in genotoxicity in HepG2 cells. In: *Journal of Physics: Conference Series* 2011, p.012037. IOP Publishing.
38. Gerloff K, Albrecht C, Boots AW, et al. Cytotoxicity and oxidative DNA damage by nanoparticles in human intestinal Caco-2 cells. 2009; 3: 355-364.
39. Horie M, Nishio K, Fujita K, et al. Cellular responses by stable and uniform ultrafine titanium dioxide particles in culture-medium dispersions when secondary particle size was 100 nm or less. 2010; 24: 1629-1638.